HHS Public Access

Author manuscript

Circ Arrhythm Electrophysiol. Author manuscript; available in PMC 2018 April 04.

Published in final edited form as:

Circ Arrhythm Electrophysiol. 2015 February ; 8(1): 193–202. doi:10.1161/CIRCEP.114.002049.

Phospholamban as a Crucial Determinant of the Inotropic Response of Human Pluripotent Stem Cell–Derived Ventricular Cardiomyocytes and Engineered 3-Dimensional Tissue Constructs

Gaopeng Chen, BS, **Sen Li, MPhil**, **Ioannis Karakikes, PhD**, **Lihuan Ren, PhD**, **Maggie Zi-Ying Chow, PhD**, **Anant Chopra, PhD**, **Wendy Keung, PhD**, **Bin Yan, PhD**, **Camie W.Y. Chan, PhD**, **Kevin D. Costa, PhD**, **Chi-Wing Kong, PhD**, **Roger J. Hajjar, MD**, **Christopher S. Chen, MD, PhD**, and **Ronald A. Li, PhD**

Cardiovascular Research Center, Icahn School of Medicine at Mount Sinai, Manhattan, NY (G.C., I.K., K.D.C., R.J.H., R.A.L.); Department of Physiology (G.C., S.L., L.R., M.Z.-Y.C., W.K., C.-W.K., R.A.L.), Stem Cell and Regenerative Medicine Consortium (G.C., S.L., L.R., M.Z.-Y.C., W.K., B.Y., C.W.Y.C., C.-W.K., R.A.L.), Department of Anatomy (C.W.Y.C.), LKS Faculty of Medicine, University of Hong Kong, Pokfulam, Hong Kong; Department of Bioengineering, Boston University, MA (A.C., C.S.C.); Harvard Wyss Institute for Biologically Inspired Engineering, Boston, MA (A.C., C.S.C.); and Department of Biology, Hong Kong Baptist University, Hong Kong (B.Y.)

Abstract

Background—Human (h) embryonic stem cells (ESCs) and induced pluripotent stem cells (iPSCs) serve as a potential unlimited ex vivo source of cardiomyocytes (CMs). However, a well-accepted roadblock has been their immature phenotype. hESC/iPSC-derived ventricular (v) CMs and their engineered cardiac microtissues (hvCMTs) similarly displayed positive chronotropic but null inotropic responses to β-adrenergic stimulation. Given that phospholamban (PLB) is robustly present in adult but poorly expressed in hESC/iPSC-vCMs and its defined biological role in β-adrenergic signaling, we investigated the functional consequences of PLB expression in hESC/iPSC-vCMs and hvCMTs.

Methods and Results—First, we confirmed that PLB protein was differentially expressed in hESC (HES2, H9)- and iPSC-derived and adult vCMs. We then transduced hES2-vCMs with the recombinant adenoviruses (Ad) Ad-PLB or Ad-S16E-PLB to overexpress wild-type PLB or the pseudophosphorylated point–mutated variant, respectively. As anticipated from the inhibitory effect of unphosphorylated PLB on sarco/endoplasmic reticulum Ca^{2+}-ATPase, Ad-PLB transduction significantly attenuated electrically evoked Ca^{2+} transient amplitude and prolonged the 50% decay time. Importantly, Ad-PLB–transduced hES2-vCMs uniquely responded to

Correspondence to Ronald A. Li, PhD, 5/F Hong Kong Jockey Club Bldg, Interdisciplinary Research, 5 Sassoon Rd, Pokfulam, Hong Kong. ronaldli@hku.hk.

The Data Supplement is available at http://circep.ahajournals.org/lookup/suppl/doi:10.1161/CIRCEP.114.002049/-/DC1.

Disclosures

None.

isoproterenol. Ad-S16E-PLB–transduced hES2-vCMs displayed an intermediate phenotype. The same trends were observed with H9- and iPSC-vCMs. Directionally, similar results were also seen with Ad-PLB–transduced and Ad-S16E–transduced hvCMTs. However, Ad-PLB altered neither the global transcriptome nor $I_{Ca,L}$, implicating a PLB-specific effect.

Conclusions—Engineered upregulation of PLB expression in hESC/iPSC-vCMs restores a positive inotropic response to β-adrenergic stimulation. These results not only provide a better mechanistic understanding of the immaturity of hESC/iPSC-vCMs but will also lead to improved disease models and transplantable prototypes with adult-like physiological responses.

Keywords

adrenergic effects; phospholamban; pluripotent stem cells; tissues

Human (h) embryonic stem cells (ESCs) can self-renew while maintaining their pluripotency to differentiate into all cell types, including cardiomyocytes (CMs).[1] Alternatively, direct reprogramming of adult somatic cells to become hES-like induced pluripotent stem cells (iPSCs) has been achieved.[2] Furthermore, directed cardiac differentiation protocols[3] are available for deriving hESC/iPSC-CMs in large quantities with yields orders of magnitude higher than the traditional method of embryoid body formation.[4] We have recently reported a method for efficient ventricular specification of hESC/iPSC.[5,6] Therefore, hESC/iPSC-CMs serve well as a potential unlimited ex vivo source of human CMs for disease modeling, drug discovery, cardiotoxicity screening, and future cell-based heart therapies.

Despite these promises of hESC/iPSC-CMs, a major roadblock has been their general lack of mature adult–like characteristics. During an action potential of native adult ventricular (v) muscle CMs, Ca^{2+} entry into the cytosol through sarcolemmal L-type Ca^{2+} ($I_{Ca,L}$) channels triggers the release of Ca^{2+} from the sarcoplasmic reticulum (SR) via the ryanodine receptors. This process, termed as Ca^{2+}-induced Ca^{2+} release,[7] escalates the cytosolic Ca^{2+} to activate the contractile apparatus for contraction. For relaxation, elevated Ca^{2+} gets pumped back into the SR by the sarco/endoplasmic reticulum Ca^{2+}-ATPase (SERCA) and extruded by the Na^{+}–Ca^{2+} exchanger to return to the resting Ca^{2+} level. Such a rise and subsequent decay of Ca^{2+}, known as the Ca^{2+} transient, modulates both the contractile force (inotropy) and beating frequency (chronotropy) of CMs. Given the central importance of Ca^{2+}-induced Ca^{2+} release in cardiac excitation–contraction coupling, proper Ca^{2+}-handling properties of hESC/iPSC-vCMs are, therefore, crucial for their clinical and other applications. Although Ca^{2+} handling of hESC/iPSC-CMs is functional, it is immature partly because of the differential developmental expression profiles of Ca^{2+}-handling proteins.[8–10] For instance, forced expression of calsequestrin, a high-capacity but low-affinity SR Ca^{2+}-binding protein whose expression is robust in adult but absent in hESC-CMs, improves Ca^{2+} transients in hESC-CMs by significantly increasing their amplitude, upstroke, and decay velocities, as well as the SR content.[9]

In the β-adrenergic signaling cascade, the activation of β-adrenergic receptors, the G protein–stimulated adenylyl cyclase and protein kinase A, leads to the phosphorylation of such substrates as phospholamban (PLB) for functional consequences in adult CMs.[11] In its

unphosphorylated form, PLB inhibits SERCA and thereby suppresses Ca^{2+} uptake into the SR; however, once PLB gets phosphorylated by protein kinase A, PLB relieves its inhibitory effect on SERCA, thereby accelerating Ca^{2+} sequestration into the SR and subsequently leading to hastened cardiac relaxation. Therefore, PLB is a crucial determinant of both myocardial contractility and β-adrenergic signaling.[11] Given that PLB is robustly expressed in adult CMs but virtually absent in hESC-CMs,[10,12] here, we investigated the functional consequences of expressing this differentially expressed gene product in single hESC/iPSC-vCMs, as well as their 3-dimensional (3D) multicellular engineered cardiac microtissues (hvCMTs).

Materials and Methods

Isolation of Human Adult Left Ventricular CMs

Human adult left ventricular CMs were isolated at UC Davis according to the protocols approved by their International Union of Pure and Applied Chemistry and Institutional Review Board (protocol numbers 200614787-1 and 200614594-1). Hearts from healthy adults of 53 to 70 years of age were digested using the Langendorff system at 37°C as we previously reported.[13]

hESC/iPSC Culture and Ventricular Specification

Undifferentiated hES2 (Wicell, Madison, WI), H9, and iPSCs (reprogrammed from $CD34^+$ cells of the peripheral blood of a normal individual)[5] were maintained on hESC-qualified Matrigel (BD Biosciences) in mTeSR1 medium (STEMCELL Technologies) as already described elsewhere.[6] For differentiation, we used a ventricular specification protocol that generates >90% hESC/iPSC-vCMs,[6,14] as gauged by the positive expression of cTnT and MLC2v, as well as their ventricular-like action potential profile. In brief, hESC/iPSC colonies were dissociated by dispase into 50 to 100 cell clusters followed by culturing in differentiation media (StemPro34, 50 μg/mL ascorbic acid and 2 mmol/L GlutaMAX-I; Invitrogen, Carlsbad, CA) supplemented with cytokines and Wnt inhibitor as follows: day 1, BMP4 (1 ng/mL) and blebbistatin (5 μmol/L); days 2 to 4.5, BMP4 (10 ng/mL) and Activin-A (5 ng/mL); days 4.5 to 7, IWR-1 (1 μmol/L) in ultralow-attachment cell culture dishes (Corning, Lowell, MA). All recombinant proteins were purchased from R&D Systems (Minneapolis, MN).

Adenoviral Gene Transfer

The cDNAs of green fluorescence protein (GFP), wild-type, and S16E-PLB[15] were subcloned into the shuttle vector pAd-RSV4. Replication deficient adenoviral (Ad) particles were packaged and amplified in HEK 293 cells by transfection with the corresponding vectors, followed by purification by the Vivapure Adenopack Kit (Vivascience) to yield titers on the order of 10^9 plaque forming units per milliliter as previously described.[16] For transducing hESC/iPSC-vCMs, cardiospheres were digested by 0.05% trypsin at 37°C for 5 minutes. Cells were seeded on coverslips and cultured in a medium containing 90% DMEM, 10% defined FBS (HyClone), 1 mmol/L of L-glutamine, and 1% of NEAA. After 48 hours, plated hESC/iPSC-vCMs were transduced by adenoviruses with a multiplicity of infection of 10 (10 plaque forming units per cell) in DMEM with 2% FBS. Our previous work showed

that a single transduction of Ad-GFP on hESC/iPSC-vCMs with 1 and 5 plaque forming units per cell yields >95% and almost 100% of positively transduced cells, respectively.[16] No noticeable morphological changes were observed after transduction. Ca^{2+} measurements and other experiments were performed 24 to 48 hours post transduction.

$I_{Ca,L}$ Measurements

$I_{Ca,L}$ was recorded from single hES2-vCMs using the whole-cell patch-clamp technique with an EPC-10 amplifier and Pulse software (Heka Elektronik) in a bath solution containing 160 mmol/L TEA-Cl, 5 mmol/L $CaCl_2$, 1 mmol/L $MgCl_2$, 10 mmol/L HEPES, 0.01 mmol/L TTX, 2 mmol/L 4-AP, and 10 mmol/L glucose (pH, 7.4) at 37°C. Patch pipette solution contained 145 mmol/L $CsCl_2$, 5 mmol/L NaCl, 2 mmol/L $CaCl_2$, 5 mmol/L EGTA, 10 mmol/L HEPES, 5 mmol/L MgATP, and pH adjusted to 7.3 with KOH.

Measurements of Cytosolic Ca^{2+}

Intracellular Ca^{2+} transients were analyzed by loading hESC/iPSC-vCMs with 2.5 μmol/L X-Rhod-1 AM (Invitrogen) for 45 minutes at 37°C in DMEM/F12, followed by imaging with a complementary metal-oxide semiconductor–based camera (MiCAM ULTIMA, SciMedia USA Ltd, CA) in Tyrode's solution containing 140 mmol/L NaCl, 5 mmol/L KCl, 1 mmol/L $CaCl_2$, 1 mmol/L $MgCl_2$, 10 mmol/L glucose, 10 mmol/L HEPES, and pH adjusted to 7.4 with NaOH. Electric stimulation or 50 mmol/L caffeine was applied to evoke Ca^{2+} transients. Isoproterenol (1 μmol/L) was incubated with hESC/iPSC-vCMs for 3 to 5 minutes at 37°C before measurement; 10 μmol/L ryanodine or 1 μmol/L thapsigargin was incubated with hES2-vCMs, as indicated, for 30 minutes at 37°C before measurements.

Microtissue Fabrication and Force Quantification

As for engineering hvCMTs,[17] polydimethylsiloxane (Sylgard 184, Dow-Corning)-microfabricated tissue gauge substrates were molded from the SU-8 masters, with embedded fluorescent microbeads (Fluoresbrite 17147; Polysciences, Inc.) on the cantilever ends. A cooled suspension of $\approx 10^6$ trypsin-digested hESC-vCMs within a reconstitution mixture, consisting of 1.5 mg/mL liquid neutralized collagen I (BD Biosciences) and 0.5 mg/mL fibrinogen (Sigma-Aldrich), was added to the substrate, and the entire assembly was centrifuged to drive the cells into the micropatterned wells. For quantifying microtissue forces, brightfield and fluorescence images were taken at 30 Hz within each template by Photometrics Evolve EMCCD camera (Photometrics). Only tissues that were uniformly anchored to the tips of the cantilevers were included in the analysis. The displacement of fluorescent microbeads at the top of the cantilevers was then tracked using the SpotTracker plug-in in ImageJ (National Institutes of Health). Four days after manufacture and tissue compaction, the microtissues were transduced by Ad-GFP, Ad-PLB, or Ad-S16E-PLB, respectively. Measurements were performed 2 days post transduction.

Western Blot

Proteins (20 μg) were electrophoresed in SDS–polyacrylamide (12%) gels. After transfer to nitrocellulose membranes, they were probed with antibodies against SERCA2a (ab2861,

Abcam), PLB (ab2865, Abcam), or β-actin (ab8226, Abcam). Detection was performed with an ECL Plus Western blotting detection system.

Real-Time Polymerase Chain Reaction

Total RNA was extracted with the RNeasy Mini kit (Qiagen). cDNAs were prepared using the SuperScript® CellsDirect cDNA Synthesis Kit (Life Technologies) following the manufacturer's protocol. Gene expressions were quantified using the StepOnePlus® Real-Time Polymerase Chain Reaction system (Applied Biosystems). Polymerase chain reaction amplifications were carried out in 96-well optical plates with SYBR® Green Polymerase Chain Reaction Master Mix (Applied Biosystems).

Immunostaining

Ad-PLB–transduced hES2-CMs were immunostained with an anti-PLB antibody (ab2865, Abcam). Primary antibodies were diluted in PBS with 1% BSA and incubated at room temperature for 1 hour. Alexa Fluor 488–conjugated goat antimouse IgGs (Invitrogen) were used as secondary antibodies and stained for 1 hour at room temperature. The cells were mounted in Prolong Gold mounting medium with DAPI (Invitrogen), and samples were imaged on LSM Carl Zeiss 510 Meta (Carl Zeiss).

Transcriptomic Analysis

Total RNAs of nontransduced, Ad-GFP–transduced, or Ad-PLB–transduced hES2-vCMs were harvested by the RNeasy Mini kit (Qiagen). The quality was confirmed by using the Agilent 2100 bioanalyzer. Expression profiles were determined by Affymetrix GeneChip Human Exon 1.0 ST Array. Data analysis was based on cell intensity files generated from the arrays using Agilent's GeneSpring GX software.

Statistical Analysis

Unless stated otherwise, all data were expressed as means±SD. Unpaired *t* test was performed to evaluate for differences between the mean values within the same study. A difference of $P<0.05$ was considered significant. For transcriptomic analysis, data were filtered with a 20% cutoff of flag value or signal intensity. Significance analysis was carried out by 1-way ANOVA with $P<0.05$ cutoff.

Results

Positive Chronotropic but Null Inotropic Responses of hvCMTs and Single hESC/iPSC-vCMs to β-Adrenergic Stimulation

Shortening of single hESC-CMs or their clusters has been measured as an index for contractile forces.[10,18] A multicellular cardiac microtissue system has been developed, where tension generated in real time can be measured.[17] Figure 1 shows that hCMTs engineered from ≈1000 hES2-vCMs each of ≈0.5 mm in length allowed continuous measurements of their spontaneous beating rate, as well as developed twitch tension under baseline control conditions. On addition of isoproterenol (10 μmol/L), a β-adrenergic agonist, the spontaneous twitch frequency increased significantly (75.6±44.6%; $P<0.01$;

n=5). However, the developed twitch tension was not altered by isoproterenol (P=0.729). These results were in complete accordance with our recent report that human ventricular cardiac tissue strips that are ≈10 mm consisting of ≈10^6 cells per tissue elicit a positive chronotropic but negligible inotropic response as gauged by their twitch forces on β-adrenergic stimulation by isoproterenol.[19] Consistent with these measurements at the tissue level, isoproterenol increased the spontaneous action potential (P=0.008; n=4) and Ca^{2+} transient firings (P=0.006; n=6) of single hES2-vCMs but not the transient amplitude (P=0.182; n=6; Figure 2). Considering the effects of frequency on the force and Ca^{2+} transients, where appropriate, the experiments that followed were electrically paced as indicated for comparison.

Effects of Ad-GFP, Ad-PLB, and Ad-S16E-PLB Transduction on the Expression Levels of PLB and SERCA of hES2-vCMs

Figure 3A shows that PLB protein was poorly expressed in hES2-vCMs compared with human adult vCMs. Adenoviral transduction of hES2-vCMs with Ad-PLB upregulated the PLB transcript and protein to levels not statistically different from those of the adult counterparts; similarly, Ad-S16E-PLB for overexpressing the pseudophosphorylated point–mutated S16E variant[15] also upregulated the PLB mRNA (Figure 3C) and protein (Figure 3B) levels in hES2-vCMs compared with those of untransduced and Ad-GFP–transduced controls. The same PLB expression trends were observed with H9-vCMs and iPSC-vCMs before and after transduction. Immunostaining of hES2-vCMs showed results consistent with this pattern (Figure 3D). By contrast, SERCA levels in all groups examined were not different (Figure 3B), suggesting a PLB-specific effect.

Effects of PLB Overexpression on the SR Load and Ca^{2+} Transient of hES2-vCMs

We next functionally characterized un transduced, Ad-GFP–transduced, Ad-PLB–transduced, and Ad-S16E-PLB–transduced hES2-vCMs. Ad-PLB–transduced hES2-vCMs displayed a significantly reduced SR Ca^{2+} load as assessed by the addition of caffeine (50 mmol/L) compared with untransduced and Ad-GFP–transduced controls (Figure 4A and 4B). As anticipated from the inhibitory effect of unphosphorylated PLB on SERCA, Ad-PLB transduction significantly attenuated the electrically evoked Ca^{2+} transient amplitude compared with untransduced and Ad-GFP–transduced controls (Figure 4C and 4D). As for the transient kinetics, both the upstroke and decay of Ad-PLB–transduced cells became significantly slow compared with controls (Figure 4E and 4F). Because Ca^{2+} influx via L-type Ca^{2+} channels modulates Ca^{2+} transients, we also examined $I_{Ca,L}$ of Ad-PLB–transduced hES2-vCMs. As shown in Figure 4G and 4H, Ad-PLB transduction did not alter $I_{Ca,L}$. Ad-S16E-PLB transduction similarly reduced the SR load and decreased the transient amplitude but to a significantly lesser extent than those of wild-type PLB (Figure 4). Thapsigargin and ryanodine, specific SERCA and ryanodine receptor inhibitors, declined Ca^{2+} transients as we previously reported.[8,9] However, Ad-PLB transduction rendered cells less sensitive to these pharmacological agents (Figure I in the Data Supplement).

Ad-PLB Transduction Restored the Positive Inotropic Response of hESC/iPSC-vCMs to β-Adrenergic Stimulation

We next investigated the effect of isoproterenol on Ca^{2+} transient in hESC/iPSC-vCMs. Isoproterenol application did not affect the Ca^{2+} transient amplitude of untransduced and Ad-GFP–transduced controls but uniquely augmented that of Ad-PLB–transduced hES2-vCMs by 69.6±47.4% (n=15; P=0.0001; Figure 5). Isoproterenol did not increase the transient amplitude of Ad-PLB-S16E–transduced cells (P=0.245). As for the 50% decay time, the Ad-PLB group was significantly reduced by isoproterenol (P=0.0001), whereas those of untransduced, Ad-GFP–transduced, and Ad-PLB-S16E–transduced cells were not changed (n=15, 15, and 25; P=0.621, 0.083, and 0.122).

Ad-PLB transduction attenuated the amplitude of Ca^{2+} transients in H9-vCMs (F/F_0=2.1±0.6, n=7 versus F/F_0=10.5±7.9, n=8 of untransduced; P=0.015) and hiPSC-vCMs (F/F_0=2.4±1.0, n=6 versus F/F_0=8.4±5.6, n=7 of untransduced; P=0.042) and prolonged their 50% decay time (H9-vCMs: 281.1±101.5 ms, n=7 versus 168.2±63.9 ms, n=8 of untransduced; P=0.0214 and iPSC-CM: 272.3±62.6 ms, n=6 versus 190.0±65.6 ms, n=7 of untransduced; P=0.042; Figure 6). Interestingly, isoproterenol increased the amplitude (H9-vCMs: F/F_0=3.3±0.8 versus F/F_0=2.4±1.0, n=7 of untransduced; P=0.013 and iPSC-CM: F/F_0=4.3±1.6 versus F/F_0=2.4±1.0, n=6 of untransduced; P=0.018) and shortened the 50% decay time (H9-vCMs: 218.0±65.2 ms versus 281.1±101.5 ms, n=7 of untransduced; P=0.048 and iPSC-CM: 208.0±84.7 ms versus 272.3±62.6 ms, n=6 of untransduced; P=0.006) of Ad-PLB–transduced H9-vCMs and hiPSC-vCMs. Taken together, these results indicated that the restoration of a positive inotropic responsiveness to β-adrenergic stimulation was specific to Ad-PLB transduction but not secondary to hESC/iPSC line-specific differences.

For further insights into this gain-of-function by Ad-PLB, we examined the global transcriptomes for potential differentially regulated genes. We performed microarray-based profiling on untransduced, Ad-GFP–transduced, or Ad-PLB–transduced hES2-vCMs. Figure 7A and 7B show that the global transcriptomes of these experimental groups were not different based on our criteria. Focused analyses on specific Ca^{2+} handling and cardiac ion channel genes also did not reveal any significant differences (Figure 7C and 7D), implicating that the functional changes observed resulted from a PLB-specific effect.

Ad-PLB Transduction Restored the Positive Inotropic Response of Ventricular Cardiac Microtissues

Although PLB overexpression restored the response of Ca^{2+} transient of single hESC/iPSC-vCMs to isoproterenol, it remained unclear whether this gain-of-function would likewise be observed at the level of force generation by multicellular 3D tissues. We, therefore, tested whether the twitch tension of hvCMTs (made out of hES2-vCMs) also responded to β-adrenergic stimulation (Figure 8A). Human vCMTs could be thoroughly transduced by Ad-GFP as demonstrated by the pattern of epifluorescence (Figure II in the Data Supplement), consistent with what we recently reported for larger engineered human cardiac tissue strips (10^6 versus 500–1000 cells). Similar to the Ca^{2+} transient amplitude of single hESC/iPSC-vCMs, the twitch tension of hvCMTs was decreased after Ad-PLB transduction (2.2±1.0

μN, n=9 versus 5.8±1.2 μN, n=4 for control; *P*=0.004). In contrast, these were not changed by either Ad-GFP or Ad-S16E-PLB (6.4±2.7 μN and 8.4±2.5 μN; n=8 and 5; *P*=0.634 and 0.186; Figure 8B). Isoproterenol application uniquely increased the twitch tension of Ad-PLB–transduced hvCMTs by 119.0±86.6% (4.5±1.9 μN; n=9; *P*=0.004) but not those of untransduced, Ad-GFP–transduced, and Ad-S16E-PLB–transduced hvCMTs (*P*=0.521; 0.164 and 0.906). However, the 50% diastolic time was unaffected in all our recordings (Figure 8C).

Discussion

Using a combination of 2D and 3D models, we reported that hESC/iPSC-vCMs and their engineered hvCMTs and cardiac tissue strips[19] similarly displayed positive chronotropic but null inotropic responses to β-adrenergic stimulation. Forced expression of PLB, which was otherwise lowly expressed in hESC/iPSC-vCMs, sufficed to restore a positive inotropic response to isoproterenol. Despite this gain-of-function, the amplitude and kinetics of immature Ca^{2+} transients, as well as the SR load of hESC/iPSC-vCMs, were further reduced by PLB overexpression. Consistently, these cellular changes were reflected at the level of multicellular tissue constructs in terms of the twitch tension of hvCMTs.

Mechanistically, Ca^{2+}-induced Ca^{2+} release ceases to operate when the SR Ca^{2+} load gets sufficiently low.[7] Despite the significant reduction of the SR content by Ad-PLB transduction, such was not observed. This reduction in the SR load likely underlies that reduced transient amplitude observed and could be attributed to the inhibitory effect of SERCA reuptake by PLB as demonstrated by the slowed decay. A decreased SR Ca^{2+} concentration in turn would negatively affect ryanodine receptor opening and therefore slow the upstroke.[20]

Adult CMs can undergo compensatory changes as a result of alterations in the environment, altering the expression or activity of certain specific gene products. Indeed, SERCA2 gene silencing has been shown to lead to remodeling of the Ca^{2+} signaling mechanisms in CMs.[21] These responses of adult CMs are generally considered adaptations for maintenance or homeostasis because, for instance, protein synthesis is largely determined by protein turnover rather than active synthesis.[21–23] By contrast, hESC/iPSC-vCMs are immature cells that robustly undergo developmental changes with active protein synthesis and regulation. Our microarray profiling showed that the global transcriptome was not altered after PLB overexpression. Therefore, the functional consequences observed after Ad-PLB transduction could be attributed to the change in PLB protein expression in hPSC-vCM per se. This notion is consistent with the known biological role in β-adrenergic signaling and Ca^{2+} handling, as supported by the intermediate effect observed with the pseudophosphorylated S16E-PLB, and further implicates that PLB plays a compartmentalized role in specific functionality, namely inotropic responsiveness to β-adrenergic stimulation and SERCA modulation in hESC-vCMs. As such, other gene products are likely responsible for global Ca^{2+}-handling maturation.

Pharmacologically (Figure I in the Data Supplement), thapsigargin, a specific SERCA inhibitor, significantly decreased the transient amplitude and slowed the decay of control and

Ad-GFP–transduced hES2-vCMs as we previously reported[8,9]; likewise, ryanodine significantly reduced the electrically evoked Ca^{2+} transient amplitude and slowed the upstroke. Interestingly, although similar inhibitory effects on the peak amplitude, decay, and upstroke by thapsigargin or ryanodine were seen with Ad-PLB–transduced hES2-vCMs, the changes were significantly less compared with the controls, indicating that Ad-PLB transduction rendered cells are less sensitive to these pharmacological agents. As anticipated from pseudophosphorylation, the effects of Ad-PLB-S16E on the responses to thapsigargin and ryanodine resembled those of controls, consistent with the notion that PLB modulates the pharmacological profile of hESC/iPSC-vCMs.

Of note, the human PLB has an amino acid difference from the rabbit isoform that was used in this study at residue K27N.[24] Experimentally, this difference has been shown to confer on human PLB a more potent ability to inhibit SERCA activity in a mouse model.[25] However, extensive studies have reported that this species-specific difference at position 27 does not affect the basal inhibitory effect on SERCA, which itself is modulated and can be unleashed by adrenergic stimulation.[25–27] Indeed, cardiac pumps and ion channels of different species are commonly studied in CMs of different species for functional and mechanistic insights.[28–30] Considering that rabbit PLB is functional, the low endogeneous expression level in hESC-CMs and the extent of restoration of chronotropic effect, it is, therefore, felt that our observations and interpretation would qualitatively remain the same.

To date, we have reported that calsequestrin 2, PLB, SERCA, and Na^{+}–Ca^{2+} exchanger are differentially expressed in hESC-CMs, fetal and adult human CMs, with defined specific roles in Ca^{2+} handling.[8,9,31,32] Partial maturation of Ca^{2+} transient properties (with an augmented amplitude, accelerated kinetics, and increased SR load) in hESC-CMs can be accomplished by overexpressing calsequestrin.[9] As demonstrated in this study, forced expression of PLB restores inotropic responsiveness, albeit other transient properties remain immature. Such incomplete maturation by engineering a single Ca^{2+}-handling gene product is perhaps not surprising and could result from the insufficient expression of specific regulatory or accessory proteins. For instance, junctin and triadin that interact with ryanodine receptor remain absent after calsequestrin transduction.[9] Similarly, Ca^{2+} handling and key ion channel transcripts are essentially unchanged after PLB overexpression. Our collective observations raise the intriguing possibility that a combinatorial approach can lead to a more mature Ca^{2+}-handling phenotype. Positive inotropic responses to adrenergic stimulation are important for adaptation[33,34]; a lack of such responses in hPSC-derived grafts could present a major obstacle to accurately model the native heart and to functional integration after transplantation. Taken together, our results not only provide a better mechanistic understanding of the immaturity of hPSC-vCMs but will also lead to better disease models and transplantable prototypes with adult-like physiological responses.

Supplementary Material

Refer to Web version on PubMed Central for supplementary material.

Acknowledgments

Sources of Funding

This work was supported by the Research Grant Council (TBRS T13-706/11 and GRF 772913), Stem Cell and Regenerative Medicine Consortium, the University of Hong Kong, and Faculty Core Facilities.

References

1. Thomson JA, Itskovitz-Eldor J, Shapiro SS, Waknitz MA, Swiergiel JJ, Marshall VS, Jones JM. Embryonic stem cell lines derived from human blastocysts. Science. 1998; 282:1145–1147. [PubMed: 9804556]
2. Takahashi K, Tanabe K, Ohnuki M, Narita M, Ichisaka T, Tomoda K, Yamanaka S. Induction of pluripotent stem cells from adult human fibroblasts by defined factors. Cell. 2007; 131:861–872. DOI: 10.1016/j.cell.2007.11.019 [PubMed: 18035408]
3. Yang L, Soonpaa MH, Adler ED, Roepke TK, Kattman SJ, Kennedy M, Henckaerts E, Bonham K, Abbott GW, Linden RM, Field LJ, Keller GM. Human cardiovascular progenitor cells develop from a kdr plus embryonic-stem-cell-derived population. Nature. 2008; 453:524–528. [PubMed: 18432194]
4. Kehat I, Kenyagin-Karsenti D, Snir M, Segev H, Amit M, Gepstein A, Livne E, Binah O, Itskovitz-Eldor J, Gepstein L. Human embryonic stem cells can differentiate into myocytes with structural and functional properties of cardiomyocytes. J Clin Invest. 2001; 108:407–414. DOI: 10.1172/JCI12131 [PubMed: 11489934]
5. Weng Z, Kong CW, Ren L, Karakikes I, Geng L, He J, Chow MZ, Mok CF, Keung W, Chow H, Leung AY, Hajjar RJ, Li RA, Chan CW. A simple, cost-effective but highly efficient system for deriving ventricular cardiomyocytes from human pluripotent stem cells. Stem Cells Dev. 2014; 23:1704–1716. DOI: 10.1089/scd.2013.0509 [PubMed: 24564569]
6. Karakikes I, Senyei GD, Hansen J, Kong CW, Azeloglu EU, Stillitano F, Lieu DK, Wang J, Ren L, Hulot JS, Iyengar R, Li RA, Hajjar RJ. Small molecule-mediated directed differentiation of human embryonic stem cells toward ventricular cardiomyocytes. Stem Cells Transl Med. 2014; 3:18–31. [PubMed: 24324277]
7. Bers DM. Cardiac excitation–contraction coupling. Nature. 2002; 415:198–205. DOI: 10.1038/415198a [PubMed: 11805843]
8. Liu J, Fu JD, Siu CW, Li RA. Functional sarcoplasmic reticulum for calcium handling of human embryonic stem cell-derived cardiomyocytes: insights for driven maturation. Stem Cells. 2007; 25:3038–3044. DOI: 10.1634/stemcells.2007-0549 [PubMed: 17872499]
9. Liu J, Lieu DK, Siu CW, Fu JD, Tse HF, Li RA. Facilitated maturation of Ca^{2+} handling properties of human embryonic stem cell-derived cardiomyocytes by calsequestrin expression. Am J Physiol Cell Physiol. 2009; 297:C152–C159. DOI: 10.1152/ajpcell.00060.2009 [PubMed: 19357236]
10. Dolnikov K, Shilkrut M, Zeevi-Levin N, Gerecht-Nir S, Amit M, Danon A, Itskovitz-Eldor J, Binah O. Functional properties of human embryonic stem cell-derived cardiomyocytes: intracellular Ca^{2+} handling and the role of sarcoplasmic reticulum in the contraction. Stem Cells. 2006; 24:236–245. DOI: 10.1634/stemcells.2005-0036 [PubMed: 16322641]
11. MacLennan DH, Kranias EG. Phospholamban: a crucial regulator of cardiac contractility. Nat Rev Mol Cell Biol. 2003; 4:566–577. DOI: 10.1038/nrm1151 [PubMed: 12838339]
12. Kong CW, Akar FG, Li RA. Translational potential of human embryonic and induced pluripotent stem cells for myocardial repair: insights from experimental models. Thromb Haemost. 2010; 104:30–38. DOI: 10.1160/TH10-03-0189 [PubMed: 20539906]
13. Poon E, Yan B, Zhang S, Rushing S, Keung W, Ren L, Lieu DK, Geng L, Kong CW, Wang J, Wong HS, Boheler KR, Li RA. Transcriptome-guided functional analyses reveal novel biological properties and regulatory hierarchy of human embryonic stem cell-derived ventricular cardiomyocytes crucial for maturation. PLoS One. 2013; 8:e77784.doi: 10.1371/journal.pone.0077784 [PubMed: 24204964]
14. Wang J, Chen A, Lieu DK, Karakikes I, Chen G, Keung W, Chan CW, Hajjar RJ, Costa KD, Khine M, Li RA. Effect of engineered anisotropy on the susceptibility of human pluripotent stem cell-derived ventricular cardiomyocytes to arrhythmias. Biomaterials. 2013; 34:8878–8886. DOI: 10.1016/j.biomaterials.2013.07.039 [PubMed: 23942210]
15. Hoshijima M, Ikeda Y, Iwanaga Y, Minamisawa S, Date MO, Gu Y, Iwatate M, Li M, Wang L, Wilson JM, Wang Y, Ross J Jr, Chien KR. Chronic suppression of heart-failure progression by a

pseudophosphorylated mutant of phospholamban via in vivo cardiac rAAV gene delivery. Nat Med. 2002; 8:864–871. DOI: 10.1038/nm739 [PubMed: 12134142]

16. Hajjar RJ, Schmidt U, Kang JX, Matsui T, Rosenzweig A. Adenoviral gene transfer of phospholamban in isolated rat cardiomyocytes. Rescue effects by concomitant gene transfer of sarcoplasmic reticulum Ca(2+)-ATPase. Circ Res. 1997; 81:145–153. [PubMed: 9242175]
17. Boudou T, Legant WR, Mu A, Borochin MA, Thavandiran N, Radisic M, Zandstra PW, Epstein JA, Margulies KB, Chen CS. A microfabricated platform to measure and manipulate the mechanics of engineered cardiac microtissues. Tissue Eng Part A. 2012; 18:910–919. DOI: 10.1089/ten.TEA.2011.0341 [PubMed: 22092279]
18. Sedan O, Dolnikov K, Zeevi-Levin N, Leibovich N, Amit M, Itskovitz-Eldor J, Binah O. 1,4,5-Inositol trisphosphate-operated intracellular Ca(2+) stores and angiotensin-II/endothelin-1 signaling pathway are functional in human embryonic stem cell-derived cardiomyocytes. Stem Cells. 2008; 26:3130–3138. DOI: 10.1634/stemcells.2008-0777 [PubMed: 18818435]
19. Turnbull IC, Karakikes I, Serrao GW, Backeris P, Lee JJ, Xie C, Senyei G, Gordon RE, Li RA, Akar FG, Hajjar RJ, Hulot JS, Costa KD. Advancing functional engineered cardiac tissues toward a preclinical model of human myocardium. FASEB J. 2014; 28:644–654. DOI: 10.1096/fj.13-228007 [PubMed: 24174427]
20. Shannon TR, Ginsburg KS, Bers DM. Potentiation of fractional sarcoplasmic reticulum calcium release by total and free intra-sarcoplasmic reticulum calcium concentration. Biophys J. 2000; 78:334–343. DOI: 10.1016/S0006-3495(00)76596-9 [PubMed: 10620297]
21. Seth M, Sumbilla C, Mullen SP, Lewis D, Klein MG, Hussain A, Soboloff J, Gill DL, Inesi G. Sarco(endo)plasmic reticulum Ca^{2+} ATPase (SERCA) gene silencing and remodeling of the Ca^{2+} signaling mechanism in cardiac myocytes. Proc Natl Acad Sci U S A. 2004; 101:16683–16688. DOI: 10.1073/pnas.0407537101 [PubMed: 15546997]
22. Seguchi M, Jarmakani JM, George BL, Harding JA. Effect of Ca^{2+} antagonists on mechanical function in the neonatal heart. Pediatr Res. 1986; 20:838–842. DOI: 10.1203/00006450-198609000-00006 [PubMed: 3748656]
23. Seguchi M, Harding JA, Jarmakani JM. Developmental change in the function of sarcoplasmic reticulum. J Mol Cell Cardiol. 1986; 18:189–195. [PubMed: 3959091]
24. Simmerman HK, Jones LR. Phospholamban: protein structure, mechanism of action, and role in cardiac function. Physiol Rev. 1998; 78:921–947. [PubMed: 9790566]
25. Zhao W, Yuan Q, Qian J, Waggoner JR, Pathak A, Chu G, Mitton B, Sun X, Jin J, Braz JC, Hahn HS, Marreez Y, Syed F, Pollesello P, Annila A, Wang HS, Schultz Jel J, Molkentin JD, Liggett SB, Dorn GW 2nd, Kranias EG. The presence of Lys27 instead of Asn27 in human phospholamban promotes sarcoplasmic reticulum Ca^{2+}-ATPase superinhibition and cardiac remodeling. Circulation. 2006; 113:995–1004. DOI: 10.1161/CIRCULATIONAHA.105.583351 [PubMed: 16476846]
26. Kimura Y, Asahi M, Kurzydlowski K, Tada M, MacLennan DH. Phospholamban domain Ib mutations influence functional interactions with the Ca^{2+}-ATPase isoform of cardiac sarcoplasmic reticulum. J Biol Chem. 1998; 273:14238–14241. [PubMed: 9603928]
27. Zhai J, Schmidt AG, Hoit BD, Kimura Y, MacLennan DH, Kranias EG. Cardiac-specific overexpression of a superinhibitory pentameric phospholamban mutant enhances inhibition of cardiac function in vivo. J Biol Chem. 2000; 275:10538–10544. [PubMed: 10744747]
28. Ennis IL, Li RA, Murphy AM, Marbán E, Nuss HB. Dual gene therapy with SERCA1 and Kir2.1 abbreviates excitation without suppressing contractility. J Clin Invest. 2002; 109:393–400. DOI: 10.1172/JCI13359 [PubMed: 11827999]
29. Tse HF, Xue T, Lau CP, Siu CW, Wang K, Zhang QY, Tomaselli GF, Akar FG, Li RA. Bioartificial sinus node constructed via in vivo gene transfer of an engineered pacemaker HCN channel reduces the dependence on electronic pacemaker in a sick-sinus syndrome model. Circulation. 2006; 114:1000–1011. DOI: 10.1161/CIRCULATIONAHA.106.615385 [PubMed: 16923751]
30. Li RA, Miake J, Hoppe UC, Johns DC, Marbán E, Nuss HB. Functional consequences of the arrhythmogenic G306R KvLQT1 K^+ channel mutant probed by viral gene transfer in cardiomyocytes. J Physiol. 2001; 533(Pt 1):127–133. [PubMed: 11351021]

31. Fu JD, Jiang P, Rushing S, Liu J, Chiamvimonvat N, Li RA. Na^+/Ca^{2+} exchanger is a determinant of excitation–contraction coupling in human embryonic stem cell-derived ventricular cardiomyocytes. Stem Cells Dev. 2010; 19:773–782. DOI: 10.1089/scd.2009.0184 [PubMed: 19719399]

32. Li S, Chen G, Li RA. Calcium signalling of human pluripotent stem cell-derived cardiomyocytes. J Physiol. 2013; 591(Pt 21):5279–5290. DOI: 10.1113/jphysiol.2013.256495 [PubMed: 24018947]

33. Laflamme MA, Chen KY, Naumova AV, Muskheli V, Fugate JA, Dupras SK, Reinecke H, Xu C, Hassanipour M, Police S, O'Sullivan C, Collins L, Chen Y, Minami E, Gill EA, Ueno S, Yuan C, Gold J, Murry CE. Cardiomyocytes derived from human embryonic stem cells in pro-survival factors enhance function of infarcted rat hearts. Nat Biotechnol. 2007; 25:1015–1024. DOI: 10.1038/nbt1327 [PubMed: 17721512]

34. Itzhaki I, Maizels L, Huber I, Zwi-Dantsis L, Caspi O, Winterstern A, Feldman O, Gepstein A, Arbel G, Hammerman H, Boulos M, Gepstein L. Modelling the long QT syndrome with induced pluripotent stem cells. Nature. 2011; 471:225–229. DOI: 10.1038/nature09747 [PubMed: 21240260]

WHAT IS KNOWN

- A key physiological feature of the heart is its ability to chronotropically and ionotropically respond to β-adrenergic stimulation.
- However, immature human pluripotent stem cell–derived cardiomyocytes display positive chronotropic but null inotropic responses.
- Phospholamban plays a defined biological role in β-adrenergic signaling.
- Phospholamban is robustly present in adult but poorly expressed in human pluripotent stem cell–derived ventricular cardiomyocytes.

WHAT THE STUDY ADDS

- Upregulation of phospholamban expression in human embryonic stem cell/induced pluripotent stem cell–derived ventricular cardiomyocytes restores a positive inotropic response to β-adrenergic stimulation.
- Not only do these results provide a better mechanistic understanding of the immaturity of human embryonic stem cell/induced pluripotent stem cell–derived ventricular cardiomyocytes but will also lead to improved disease models and transplantable prototypes with adult-like physiological responses.

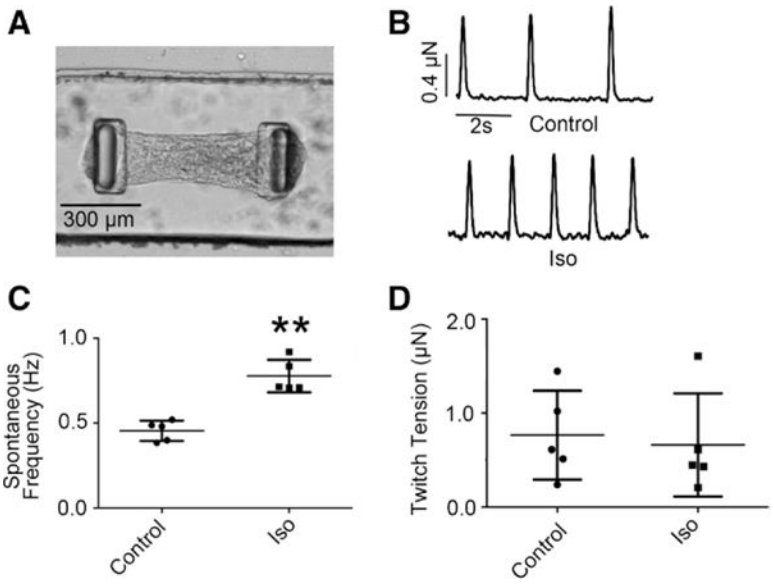

Figure 1.

Positive chronotropic but null inotropic responses of hES2-derived ventricular microtissues (hvCMTs) to β-adrenergic stimulation. **A**, Image of a typical hvCMT on a microfabricated tissue gauge device. **B**, Representative raw tracings of hvCMT at the baseline (upper) and after 10 μmol/L isoproterenol (Iso) treatment (down). **C**, Iso increased the spontaneous twitch frequency (n=5; ** P<0.01). **D**, Iso did not affect the developed twitch tensions (P=0.729).

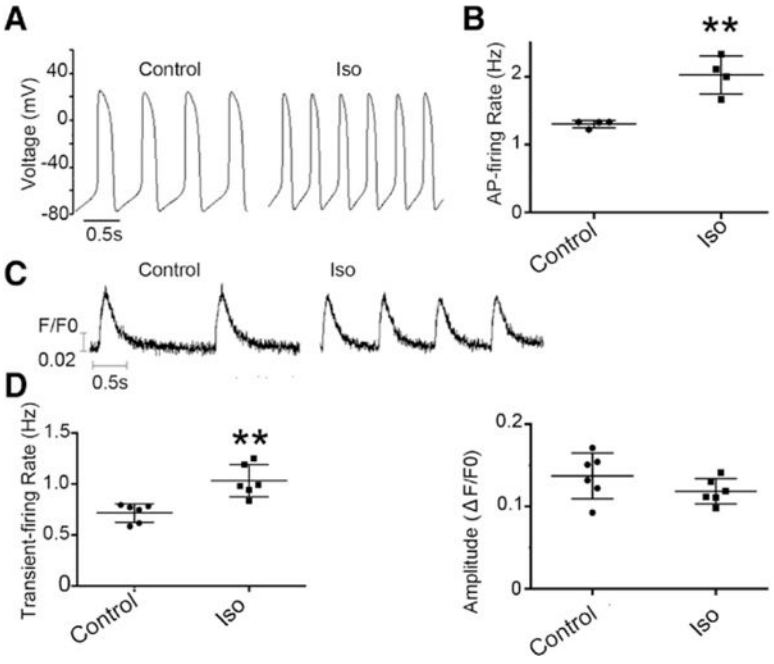

Figure 2.

Isoproterenol (Iso) increased the spontaneous action potential (AP) and Ca^{2+} transient firings (chronotropy) of single hES2-ventricular microtissues (vCMs) but not the transient amplitude. **A**, Representative AP tracings of single hES2-vCMs before and after Iso. **B**, The corresponding AP firing frequencies (n=4; ** P=0.008). **C**, Representative recordings of spontaneous Ca^{2+} transients. **D**, Transient rate (** P=0.005) and amplitude (P=0.182) of Ca^{2+} transients (n=6).

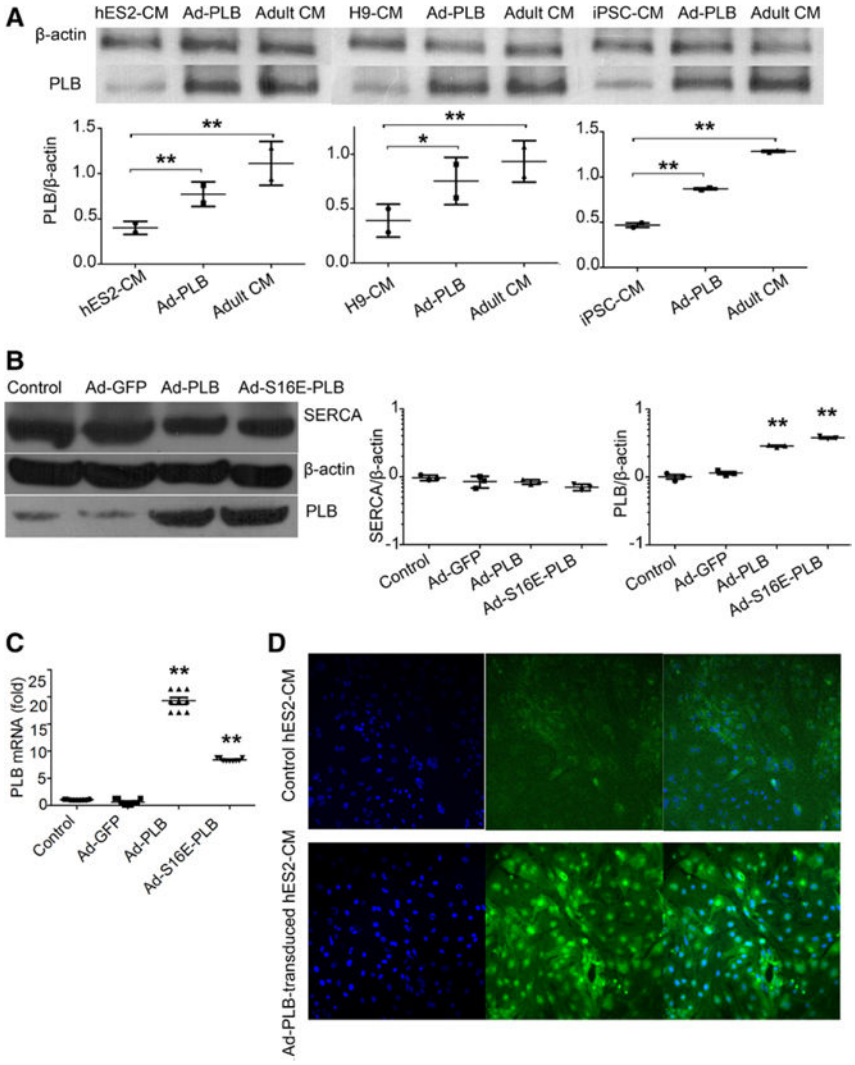

Figure 3.

Effects of adenovirus (Ad)-green fluorescence protein (GFP), Ad-phospholamban (PLB), and Ad-S16E-PLB transduction on the expression levels of PLB, sarco/endoplasmic reticulum Ca^{2+}-ATPase (SERCA). **A**, Western blot showing Ad-PLB transduction increased PLB protein expression in hES2-ventricular cardiomyocytes (vCMs; **left**), H9-vCMs (**middle**), and induced pluripotent stem cell (iPSC)-vCMs (**right**) but did not reach the adult level (n=2; *P*=0.226, 0.644, and 0.001 for hES2-vCMs, H9-vCMs, and iPSC-vCMs). **B**, Western blot analysis shows that the PLB protein levels of the Ad-PLB and Ad-S16E-PLB groups were significantly increased, but those for SERCA were not different from the untransduced and Ad-GFP–transduced groups (n=3). **C**, PLB transcript levels as gauged by quantitative polymerase chain reaction (n=3). **D**, Immunostaing images show that Ad-PLB–transduced hES2-vCMs were 100% positive: cell nucleus indicated by DAPI (**left**), PLB staining (**middle**), and merged image (**right**).

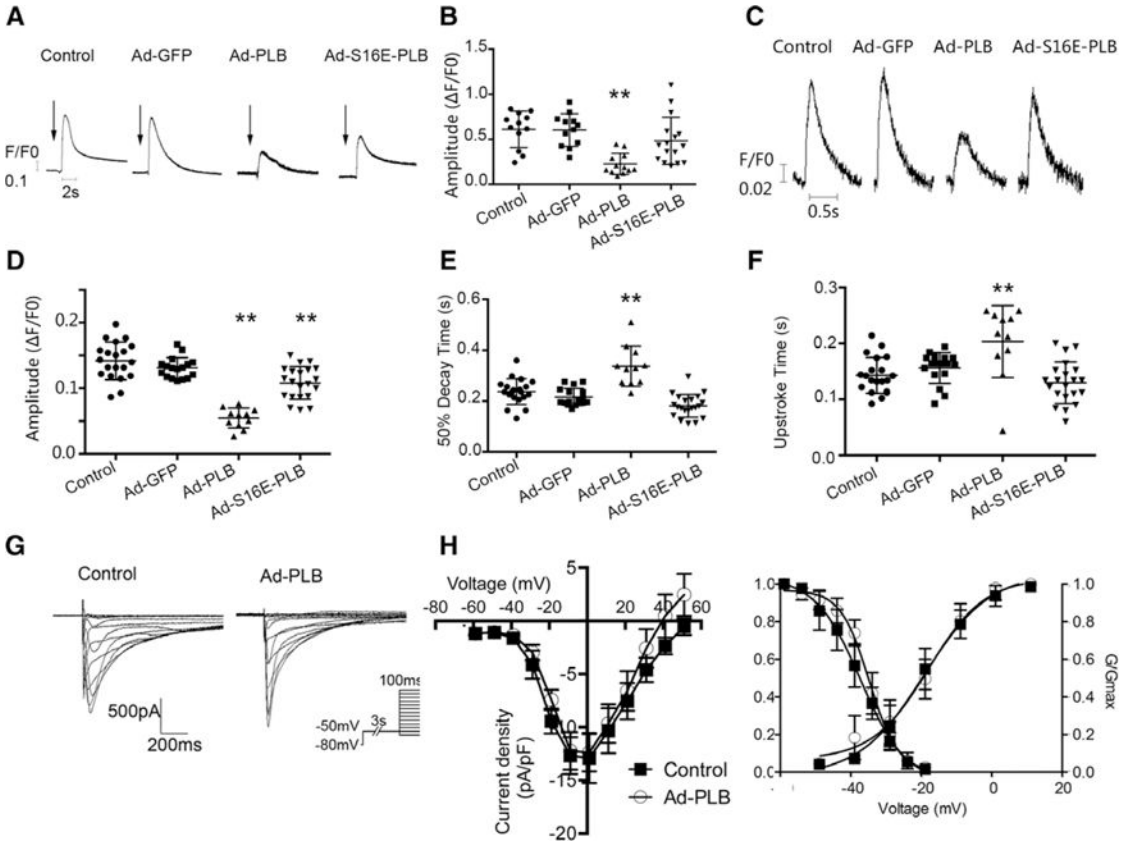

Figure 4.

Effects of adenovirus (Ad)-green fluorescence protein (GFP), Ad-phospholamban (PLB), and Ad-S16E-PLB transduction on the Ca^{2+} transient properties, SR load, and $I_{Ca,L}$ of hES2-ventricular cardiomyocytes (vCMs). **A**, Representative raw tracings of caffeine-induced Ca^{2+} transients (arrows indicate the time of caffeine application). **B**, Bar graphs summarizing the amplitudes of the same groups as indicated. Ad-PLB transductions significantly decreased the sarcoplasmic reticulum (SR) load (n=11, 11, 11, and 15 for control, Ad-GFP, Ad-PLB, and Ad-S16E-PLB, respectively). Untransduced vs Ad-S16E-PLB–tranduced: P=0.17. **C**, Representative raw tracings of electrically induced Ca^{2+} transients of untransduced, Ad-GFP–transduced, Ad-PLB–transduced, and Ad-S16E-PLB–transduced hES2-vCMs paced at 1 Hz. **D–F**, Bar graphs summarizing the transient parameters of the same groups from **C**. Ad-PLB transduction significantly decreased the transient amplitude (**D**) and prolonged the 50% decay (**E**) and upstroke (**F**). Ad-S16E-PLB transduction produced an intermediate phenotype (n=20, 17, 11, and 21 for control, Ad-GFP, Ad-PLB, and Ad-S16E-PLB. Untransduced vs Ad-S16E-PLB–tranduced: P=0.29 for upstroke time, P=0.14 for 50% decay time, and ** P<0.01, compared with control. **G** and **H**, Representative $I_{Ca,L}$ tracings of nontransduced and Ad-PLB–transduced hES2-vCMs. Electrophysiological protocol is given in the inset. Current density (I)–voltage (V) plots and steady-state activation curves revealed no significant differences. n=7 and 5 for control and Ad-PLB–transduced CMs, respectively.

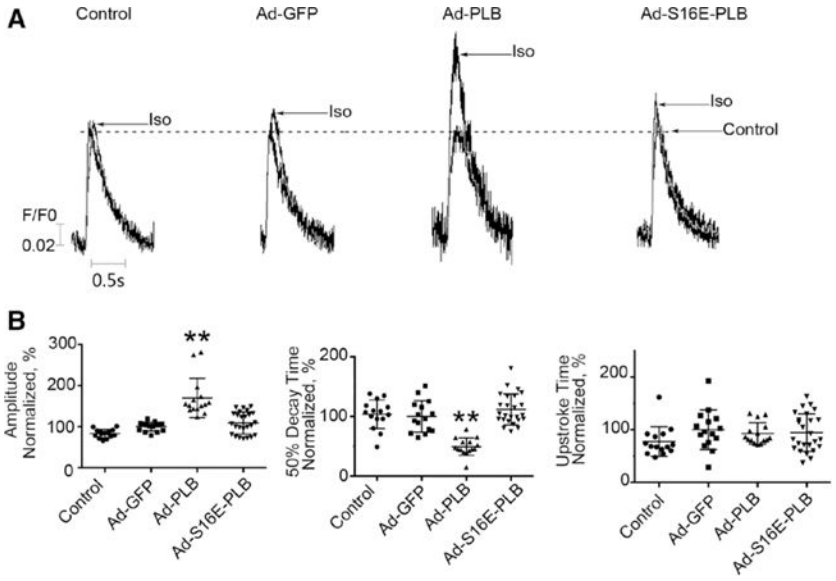

Figure 5.

Restoration of a positive inotropic response of hES2-ventricular cardiomyocytes (vCMs) by phospholamban (PLB) overexpression. **A**, Representative raw tracings of electrically induced Ca^{2+} transients of untransduced, adenovirus (Ad)-green fluorescence protein (GFP)–transduced, Ad-PLB–transduced, and Ad-S16E-PLB–transduced human embryonic stem cell (hESC)–derived vCMs paced at 1 Hz recorded in the absence and presence of isoproterenol (Iso) as indicated. Peaks recorded under control drug–free condition of all groups have been normalized for comparison. **B**, Bar graphs summarizing the transient parameters of the same groups from (**A**). Ad-PLB–transduced hESC-vCMs uniquely responded to Iso (n=15, 15, 15, and 25 for control, Ad-GFP, Ad-PLB, and Ad-S16E-PLB respectively; $^{**}P<0.01$, compared with parameters under drug-free condition).

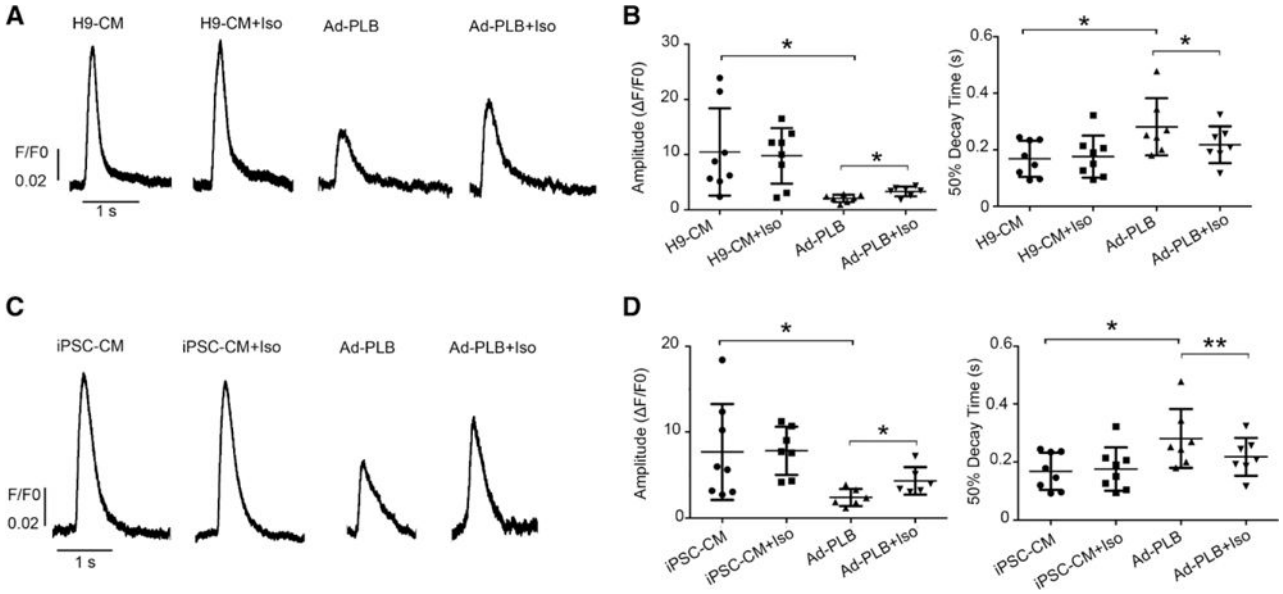

Figure 6.

Restoration of a positive inotropic response of human (H)9-ventricular cardiomyocytes (vCMs) and induced pluripotent stem cell (iPSC)–derived vCMs by phospholamban (PLB) overexpression. **A**, Representative raw tracings of electrically induced Ca^{2+} transients of untransduced or adenovirus (Ad)-PLB–transduced H9-CMs paced at 0.5 Hz with/without isoproterenol (Iso) application. **B**, Bar graphs summarizing amplitude and 50% decay time of the same groups from **A** (n=8 and 7 for untransduced or Ad-PLB–transduced H9-CMs). **C**, Representative raw tracings of electrically induced Ca^{2+} transients of untransduced or Ad-PLB–transduced iPSC-CMs paced at 0.5 Hz with/without Iso. **D**, Bar graphs summarizing amplitude and 50% decay time of the same groups from **C** (n=7 and 6 for untransduced or Ad-PLB–transduced iPSC-CMs; *P<0.05 and **P<0.01).

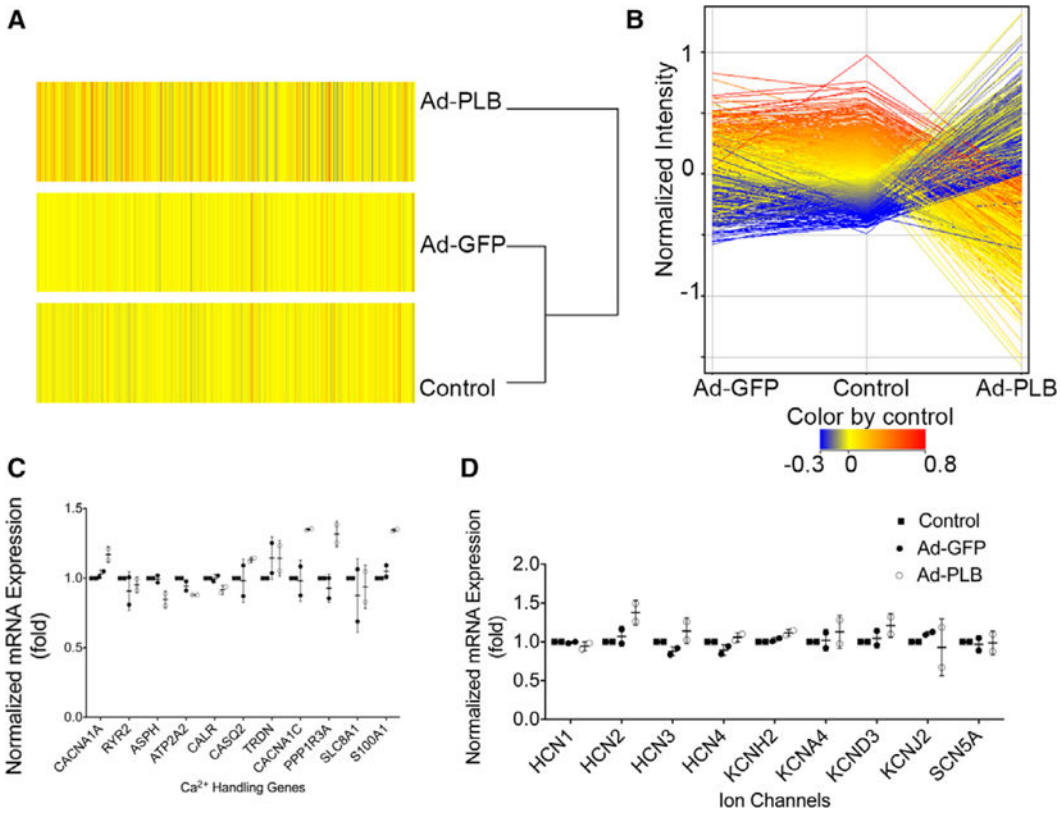

Figure 7.

Transcriptomic analysis. **A**, Heat maps of microarray transcriptomic profiling of untransduced, adenovirus (Ad)-green fluorescence protein (GFP)–transduced, and Ad-phospholamban (PLB)–transduced human embryonic stem cell–derived ventricular cardiomyocytes. **B**, No significant changes in the global gene expression or those of (**C**) calcium-handling genes and (**D**) or ion channels were detected (n=2).

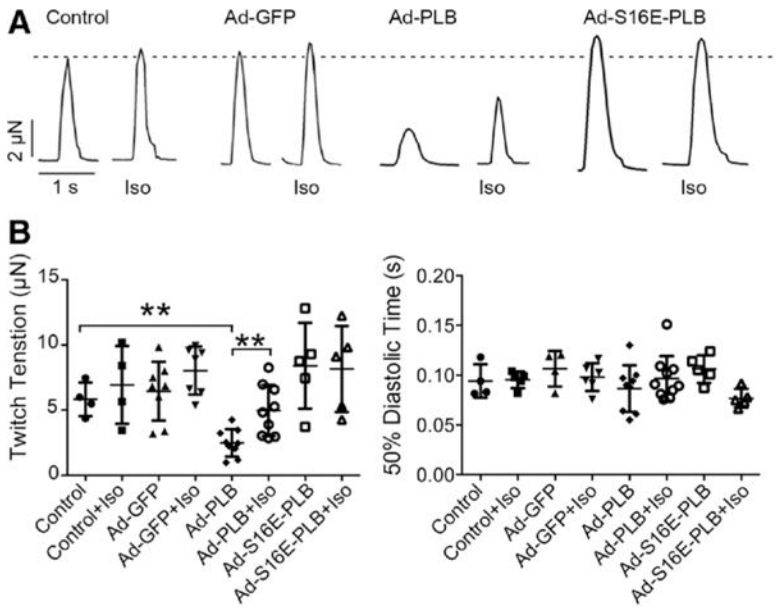

Figure 8.

Restoration of a positive inotropic response in engineered cardiac microtissues (hvCMTs) by phospholamban (PLB) overexpression. Adenovirus (Ad)-PLB transduction uniquely attenuated the developed tensions of hvCMTs but restored a positive inotropic response to isoproterenol (Iso). **A**, Raw tracings of untransduced, Ad-green fluorescence protein (GFP)–transduced, Ad-PLB–transduced, and Ad-S16E-PLB–transduced hvCMTs recorded paced at 0.5 Hz in the absence and presence of Iso as indicated. The dotted line shows the peak of untransduced hvCMT recorded under Iso-free condition. **B**, Bar graph summarizing the twitch tension (the dotted line shows twitch tension of untransduced hvCMTs recorded under Iso-free condition) and 50% diastolic time from the same groups (n=4, 8, 9, and 5 for control, Ad-GFP, Ad-PLB, and Ad-S16E-PLB, respectively; $^{**}P<0.01$).